



**Get Clarity On Generics**

Cost-Effective CT & MRI Contrast Agents



FRESENIUS  
KABI

WATCH VIDEO

**AJNR**

This information is current as  
of August 6, 2025.

**Visualization of Nonstructural Changes in  
Early White Matter Development on  
Diffusion-Weighted MR Images: Evidence  
Supporting Premyelination Anisotropy**

Daniela Prayer, A. James Barkovich, Daniel A. Kirschner,  
Lukas M. Prayer, Timothy P.L. Roberts, John Kucharczyk  
and Michael E. Moseley

*AJNR Am J Neuroradiol* 2001, 22 (8) 1572-1576  
<http://www.ajnr.org/content/22/8/1572>

# Visualization of Nonstructural Changes in Early White Matter Development on Diffusion-Weighted MR Images: Evidence Supporting Premyelination Anisotropy

Daniela Prayer, A. James Barkovich, Daniel A. Kirschner, Lukas M. Prayer, Timothy P.L. Roberts, John Kucharczyk, and Michael E. Moseley

**BACKGROUND AND PURPOSE:** Previously, we showed that diffusion-weighted MR imaging depicts evidence of directionally preferential water motion in white matter structures of developing rat brain before and after myelination, and considerably earlier than conventional imaging strategies. Present data augment these imaging and corresponding histologic findings with electron-microscopic corroboration. We additionally report the findings of a 10-day-old rat pup tested functionally by administration of the sodium-channel blocker, tetrodotoxin.

**METHODS:** In two rat pups, drawn from the population reported previously, MR estimates of diffusion anisotropy of the optic nerves and chiasm were compared with histologic and electron microscopy results. To test the hypothesis that “premyelination” directional preference of water motion in white matter structures relates to sodium-channel activity, MR imaging was performed in a 10-day-old rat pup treated with the sodium-channel blocker, tetrodotoxin, and findings were compared with data from an age-matched control.

**RESULTS:** Although diffusion anisotropy was present in optic structures of the youngest animal, myelin-sensitive histologic staining did not show myelin before 12 days; electron microscopy confirmed lack of any myelin or its precursors during the earliest maturational stage. Administration of tetrodotoxin to the 10-day-old rat-pup led to loss of diffusion anisotropy.

**CONCLUSION:** Our findings provide two pieces of supporting data for the hypothesis that nonstructural changes are responsible for early anisotropic diffusion: electron microscopy shows no evidence of myelin despite diffusion anisotropy, and inhibiting the sodium-channel pump appears to remove the directional preference of water motion. Visualization of nonstructural “premyelination” consequences with diffusion-weighted imaging emphasizes its sensitivity and potential in studying early processes of brain development.

The rate and direction of diffusion of water protons in a tissue matrix reflect both osmotic forces and molecular barriers or other hindrances encountered during an experimental observation time. This re-

lationship is approximated by the apparent diffusion coefficient (ADC)-modified Einstein equation that defines the components of the ADC along any direction as  $L^2 = 2(\text{ADC})T$ , where  $L$  is the distance traveled in a certain direction and  $T$  is the observation time. Diffusion of water protons causes spin dephasing in an appropriate MR imaging experiment (1). Such diffusion can be exploited in imaging studies, as the resultant spin dephasing leads to signal loss proportionate to the amount of diffusion. If the components of the ADC in different directions are unequal (ie, there is a “preferred” direction of water motion), diffusion is termed “anisotropic.” Of particular relevance in white matter tracts, diffusion parallel to the axons is relatively “free” (a high ADC value), whereas perpendicular components of the ADC are lower.

The degree of diffusion anisotropy relates to the development of myelination (2). Although it was

---

Received February 29, 2000; accepted after revision March 19, 2001.

From the Department of Radiology (D.P., L.M.P.), Section of Neuroradiology, University of Vienna, Austria; Department of Radiology (D.P., A.J.B., L.M.P., T.P.L.R., J.K.), Neuroradiology Section, University of California at San Francisco; Department of Biology (D.A.K.), Boston College, Chestnut Hill, Massachusetts; Department of Radiology (M.E.M.), Stanford University, Palo Alto, California.

The authors gratefully acknowledge the Max Kade Foundation for the support of this work.

Address reprint requests to Tim Roberts, PhD, Department of Radiology, Box 0628, University of California at San Francisco, 513 Parnassus Avenue, San Francisco, CA 94143.

© American Society of Neuroradiology

postulated initially that the myelin sheaths are solely responsible for the hindrance of proton diffusion across the axon (3), it recently has been shown that diffusion anisotropy can be seen even in white matter tracts that appear unmyelinated on light microscopy (4). Our previous work suggested that "premyelination" processes, such as activity of the sodium channel, might be responsible for the observed anisotropic water diffusion in the white matter of the developing rat brain, despite the absence of MR imaging or histologic evidence of myelin itself.

The present communication reports two pieces of data, relating to our previous studies of anisotropic diffusion in the developing rat pup, which support the nonstructural explanation of diffusion anisotropy in early stages of white matter development and point explicitly to the role of sodium-channel activity in directionally preferential water motion.

## Methods

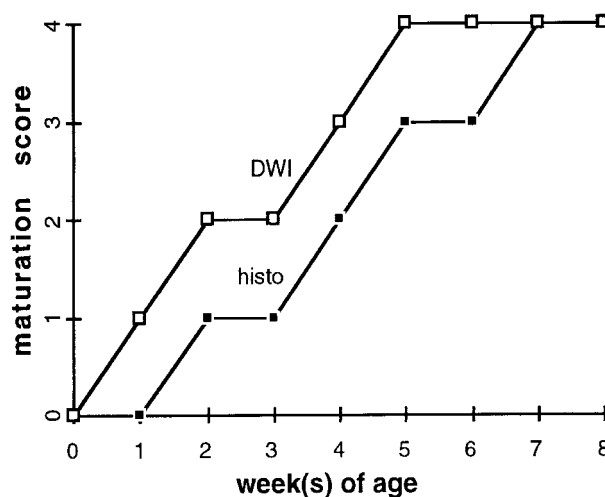
### MR Imaging

The MR imaging studies were performed on a GE-Omega CSI scanner (General Electric, Milwaukee, WI), operating at 4.7 T, as described (4). In brief, diffusion-weighted (TR/TE 2000/80 ms, b value  $\sim 1300$  s/mm<sup>2</sup>) spin-echo images were acquired (5). Two sets of images were obtained with diffusion sensitizing gradients applied in orthogonal directions. The z gradient was approximately parallel to the orientation of the optic nerves and tracts; the y direction was perpendicular to them. Diffusion anisotropy was assessed on a voxel-by-voxel basis by constructing a ratio of intensities from images with equal b values but orthogonal-direction sensitivities. The ratio of intensity from each voxel was used to construct ratio images that are spatial maps ("diffusion anisotropy maps") representing the relative amount of diffusion anisotropy in each location. This approach detects important manifestations of anisotropic diffusion without the requirement for a more thorough, full-matrix, tensor approach. This approach, commonly referred to as diffusion tensor imaging (DTI), has a substantial time penalty, prohibiting application in our experimental model with neonatal rat pups. We speculate that a full DTI approach, had it been applied, would have been no less and likely even more sensitive to anisotropy itself and thus would have revealed evidence of anisotropy at an even earlier developmental stage.

### Evaluation

Anisotropy ratio images (anisotropy "maps") and histologic sections were evaluated for signal intensity, degree of staining, and proof of myelinated axons (6). Data from the other rat pups in the cohort (4) were reevaluated according to the same criteria.

Criteria for white matter maturation were signal increase on calculated anisotropy maps, increasing diameter of the optic nerve, or both. We adopted a four-stage classification of the maturation process: maturation was considered to start at the very time point of the first signal changes (first grade of maturation); progress in maturation was defined by increasing brightness on diffusion anisotropy maps or an increasing diameter of the optic nerve (second grade). The presence of both increased hyperintensity on anisotropy maps and increased diameter characterized the third grade of maturation. When all signal characteristics remained completely unchanged on all



DWI.....diffusion-anisotropy maps

histo.....results of histological staining

FIG 1. Maturation score defined according to anisotropic diffusion-weighted imaging and histologic sections, respectively, as a function of rat pup postnatal age. Anisotropy of diffusion precedes, by about 1 week, histologic evidence of myelin in the optic nerves, internal capsules, and corpus callosum.

further MR examinations, the maturation process was considered complete (fourth grade of maturation). For assessment of histologic maturation, the intensity of staining and diameter of the optic nerve were used as grading criteria.

### Electron Microscopy

In two rat pups (7 days and 21 days old) from the previously reported cohort (4), the optic nerves were fixed for electron microscopy in 1.5% glutaraldehyde in 0.08 mol/L phosphate buffer (Sorenson's buffer) at pH 7.2 for 2 hours at room temperature. After two 10-minute washes in buffer, the nerves were post-fixed for 1 hour in 1% osmium tetroxide, dehydrated in an alcohol series to propylene oxide, infiltrated overnight with 50:50 propylene oxide:Epon, and embedded in pure Epon resin at 70°C under vacuum. Thick sections (2  $\mu$ m) were cut using a Reichert-Jung 2050 ultramicrotome and stained with 1% toluidine blue dissolved in 1% sodium borate and 70% ethanol. Thin sections (60–90 nm) were cut using an LKB 8800 ultratome 111 with a diamond knife and stained with 5% uranyl acetate in 50% ethanol for 5 minutes and Reynolds's lead citrate for 2 minutes. The sections were examined in a JEOL 1200EX electron microscope operating at 120 kV.

### Functional Testing

Specifically to investigate the influence of sodium-channel activity on early diffusion anisotropy, the sodium-channel blocker tetrodotoxin (TTX) (7, 8) was given intraperitoneally at a dose of 0.1  $\mu$ g/10 g to a 10-day-old rat pup. This treated rat pup and an untreated sibling (age-, weight-, and sex-matched) were then imaged and diffusion anisotropy maps were constructed.

## Results

Reevaluating the anisotropic diffusion maps and histologic sections in terms of white matter maturational stage (Fig 1) confirmed our previous find-

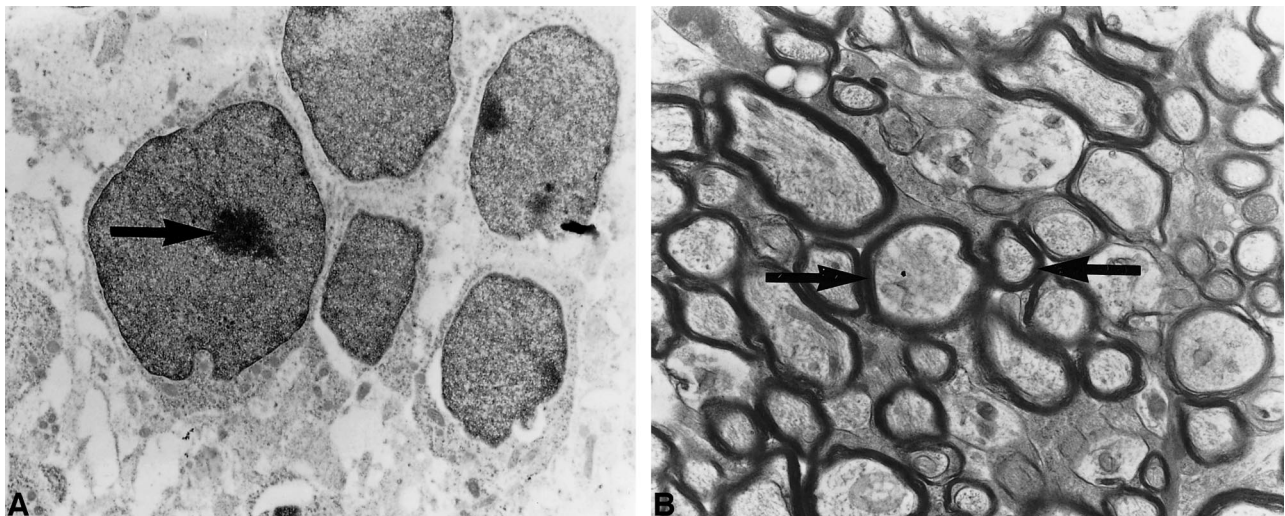


FIG 2. Electron-microscopy preparation of the optic nerve of a 7-day-old rat pup (A) shows no evidence of myelin sheaths or significant structural changes within the oligodendrocytes. Oligodendroglial cells have large nuclei (black arrow). Electron-microscopy preparation of the optic nerve of a 21-day-old rat pup (B) shows myelin sheaths (black arrows) surrounding multiple axons.

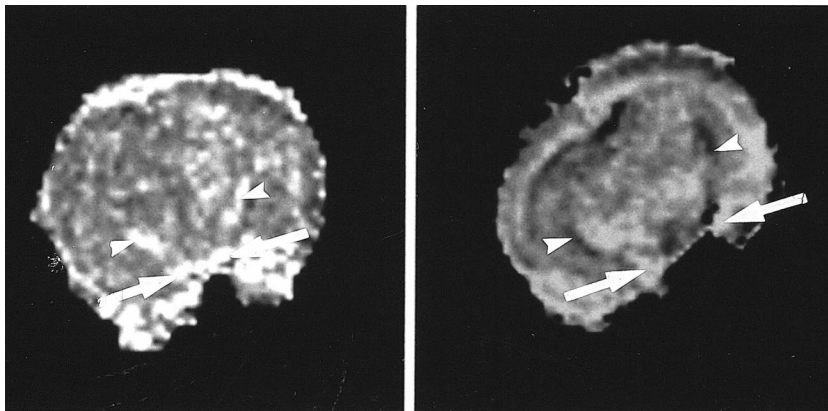


FIG 3. Coronal diffusion anisotropy maps of 10-day-old rat pups, showing the effect of tetrodotoxin (TTX). The untreated animal (left) shows high signal intensity in the slightly myelinated optic structures (white arrows), and the unmyelinated internal capsules (white arrowheads) show diffusion anisotropy. In the TTX-treated animal (right), diffusion anisotropy is no longer visible in the unmyelinated internal capsule. However, anisotropy (hyperintensity) still is present in the partially myelinated optic nerves, presumably because the hydrophobic myelin sheath already constitutes a physical barrier to water diffusion. This suggests that the anisotropy present before myelin results from a physiological phenomenon, such as sodium diffusion, that is paralyzed by the TTX. Note that the intensity of the entire TTX-treated brain appears different from that of the untreated animal. This intensity change is attributed to TTX-induced global cytotoxic edema, restricting water motion in gray matter as well as white matter.

ings (4) that anisotropy of diffusion precedes histologic evidence of myelin in the optic nerves, internal capsules, and corpus callosum.

#### *Electron Microscopy Results*

The optic nerve of the 7-day-old animal showed no myelinated fibers, only oligodendroglial cells with prominent nuclei surrounded by thin rims of cytoplasm. Axons were poorly differentiated from the surrounding tissue (Fig 2A). The optic nerve of the 21-day-old showed numerous myelinated axons, with the smaller caliber axons having thinner sheaths and the larger axons having thicker myelin sheaths (Fig 2B).

#### *Functional Results*

Diffusion anisotropy was shown in the optic nerves and tracts, but not in the internal capsule, of the TTX-treated rat (Fig 3). In contrast, anisotropy was shown in both the optic structures and the internal capsules of the control pup, which was not treated with TTX (Fig 3).

#### *Discussion*

When diffusion-weighted MR imaging first showed anisotropic diffusion in white matter, it was believed to result entirely from myelination (1). However, an investigation comparing the onset and progression of diffusion anisotropy of several white



matter tracts with the evolution of myelination, as assessed by light microscopy of rat pup brains stained for myelin, revealed that the onset of diffusion anisotropy preceded detection of myelin stain by 5 to 12 days (4). In the present study, the onset of diffusion anisotropy before myelination was confirmed by electron microscopy; no evidence of myelination was found on electron microscopy sections of the optic nerves of the 7-day-old rat pup, although diffusion anisotropy had been shown by MR imaging in rat pups as young as 5 days old. The axons in animals of this age are in the so-called "premyelinating" state (9, 10).

At present, we can only speculate about the nature of premyelination events within the axon that cause anisotropic water diffusion. However, the microbiological changes that precede cerebral myelination have been the object of several detailed investigations (9, 11–13). The structural and functional alterations of axons and oligodendrocytes that may contribute to diffusion anisotropy include increase of the axonal diameter, increase in the concentration of microtubule-associated proteins and microperoxisomes, membrane additions to the axolemma, increasing density of sodium channels, and onset of activity of  $\text{Na}^+/\text{K}^+$ -ATPase; these have been discussed previously (4). It also has been shown, by means of ion-sensitive microelectrodes (14) and iontophoresis (15), that brain tissue behaves like an anisotropic, porous medium in which the extracellular domain is a channel for diffusion of different molecules and ions. A theoretical model for water diffusion in tissues has emphasized the role of extracellular volume fraction and intracellular diffusion in altering the ADC (16). These results and concepts form the basis for the following discussion.

In our experiments, electron microscopy of the 7-day-old animal revealed no structural changes of the axons or oligodendrocytes that are known to characterize premyelination (4, 9–11, 17–23). These findings support the hypothesis that anisotropic diffusion at this stage is mainly due to functional changes (4).

The fractional volume and tortuosity of the extracellular space (both of which reflect the presence of microparticles and membranes known to hinder diffusion) have been shown to remain constant in the white matter of rat pups younger than 10 to 11 days (24). Dramatic reduction of the fractional volume occurs between postnatal days 10 and 21 (24). These observations indicate a lack of accumulation of structures in the extracellular space during the first postnatal week; thus, "myelination gliosis" (4, 17) and other extracellular structural changes are unlikely related to the generation of early diffusion anisotropy.

Premyelination changes of the axon include an increase in the density of sodium channels in regions of astrocytic contact with the axon immediately before myelin ensheathment (11). Premyelinated axons of the optic nerve possess a density of

sodium channels of  $2/\text{mm}^2$ , sufficient to support the genesis of electrical action potentials, probably due to the high-input resistance (13). It has been shown that axonal electrical activity at this stage of development controls the production or release of the growth factors responsible for the proliferation of oligodendrocyte precursor cells (25, 26). The same mechanism has been implicated in the process of axonal recovery in demyelinating diseases (27). As a result of this observation, and the fact that sodium channels increase by a factor of 4 in lesions of multiple sclerosis (28), some have suggested that remyelination might recapitulate the principal events of developmental myelinogenesis (27). These suggestions are emphasized by the fact that oligodendrocyte progenitors are present in the lesions of multiple sclerosis in adults (29).

Factors that determine the rate of movement of water molecules across a barrier include transbarrier concentration differences, the thickness of the barrier, barrier permeability, and resistance to water diffusion across the barrier. Moreover, electrochemical differences across the barrier, caused by the presence of ions such as  $\text{Na}^+$ ,  $\text{K}^+$ , and  $\text{Cl}^-$ , may induce passive transbarrier water movement. In myelinated axons, the  $\text{Na}^+/\text{K}^+$ -ATPase pump and the  $\text{Na}^+-\text{H}^+$  antiporter mechanisms keep the intracellular compartments 60–90 mV negative relative to the extracellular fluid (30). The parallel development of intraaxonal macromolecules (20–22) and functional ionic channels derives from the need of the axon to maintain its volume. The osmotic pressure of intracellular, impermeable anions attracts positively charged cations, mainly sodium, which must be balanced and compensated by active sodium extrusion by the  $\text{Na}^+/\text{K}^+$  pump (31). As bulk water moves together with sodium, this mechanism favors the movement of water molecules from intraaxonal to extraaxonal compartments and thus will render the diffusion into or through (but not along) the axon more difficult (4).

It has been shown that TTX-sensitive sodium channels are responsible for the generation of action potentials in myelinated and unmyelinated axons (26, 29). To test whether sodium-channel activity contributes to early diffusion anisotropy, TTX was given to a 10-day-old rat pup for selective blockade of the sodium channels (7, 8). Because the optic nerve, but not the axons of the internal capsule, are myelinated at 10 days (9), we expected measurable anisotropy in the optic nerve but none in the internal capsule after TTX administration. Diffusion anisotropy was indeed shown in the optic nerve and tracts, but not in the internal capsule of the treated rat (Fig 3). In comparison, anisotropy was evident in both the optic structures and the internal capsules of the untreated rat. The absence of capsular anisotropy in the treated rat, combined with the presence of anisotropy in the untreated rat, supports our hypothesis that ionic channel activity in the premyelination state contributes to diffusion anisotropy. Support also is added

by the observation that reductions in the mean ADC are measured in the optic radiations after photic stimulation; ie, increased activity within the axon reduces diffusion (32, 33).

Sodium-channel blockade by antibodies recently has been shown as the probable mechanism for axonal dysfunction in demyelinating disorders such as Guillain-Barré syndrome and multiple sclerosis (27, 34), raising the index of suspicion that sodium channels may be targets of immune attack in some neurologic disorders (34). It also has been shown that remyelination is not essential for remission in demyelinating diseases such as multiple sclerosis (28, 34, 35). Restoration of axonal function has been ascribed to a normal  $\text{Na}^+/\text{K}^+$  conductance ratio (27).

## Conclusion

Our findings suggest that diffusion anisotropy during "premyelinating" states does not have a morphologic correlate either in light microscopy or in electron microscopy. In addition, evidence strongly suggests that ionic fluxes secondary to action potentials result in directional water diffusion in the absence of myelination. The ability of diffusion-weighted imaging to depict changes generated by these action potentials might be helpful in the early detection of both myelination disorders and axonal recovery and potential remyelination in patients with demyelinating disorders, before the presence of structural changes.

## References

- Moseley M, Cohen Y, Kucharczyk J, et al. **Diffusion-weighted MR imaging of anisotropic water diffusion in cat central nervous system.** *Radiology* 1990;176:439-445
- Sakuma H, Nomura Y, Takeda K, et al. **Adult and neonatal human brain: diffusional anisotropy and myelination with diffusion-weighted MR imaging.** *Radiology* 1991;180:229-233
- Rutherford M, Cowan F, Manzur A, et al. **MR imaging of anisotropically restricted diffusion in the brain of neonates and infants.** *J Comput Assist Tomogr* 1991;15:188-198
- Wimberger D, Roberts T, Barkovich AJ, Prayer DC, Moseley ME, Kucharczyk J. **Identification of "premyelination" by diffusion-weighted MRI.** *J Comput Assist Tomogr* 1995;19:28-33
- Le Bihan D, Turner R, Mac Fall JR. **Effects of intravoxel incoherent motions (IVIM) in steady-state free precession (SSFP) imaging: application to molecular diffusion imaging.** *Magn Reson Med* 1989;10:324-337
- Carson F. **Myelin staining methods.** In: Sheehan D, Hrapchak B, eds. *Theory and Practice of Histotechnology*. St. Louis, Mo: Mosby; 1980:252-264
- Catterall W, Beneski D. **Biochemical and allosteric properties of neurotoxin receptor sites associated with voltage-sensitive sodium channels.** In: Matsumoto G, Kotani M, eds. *Nerve Membrane. Biochemistry and Function of Channel Proteins*. Tokyo: University of Tokyo Press; 1981:3-11
- Stys PK, Waxmann SG, Ransom BR. **Ionic mechanism of anoxic injury in mammalian white matter: role of  $\text{Na}^+$  channels and  $\text{Na}^+ \text{Ca}^{2+}$  exchanger.** *J Neuroscience* 1992;12:430-439
- Hildebrand C, Waxman S. **Postnatal differentiation of rat optic nerve fibers: electron microscopic observations on the development of nodes of Ranvier and axoglial relations.** *J Comp Neurol* 1984;224:25-37
- Black JA, Waxman SG, Ransom BR, Macariod DE. **A quantitative study of developing axons and glia following altered gliogenesis in rat optic nerve.** *Brain Res* 1986;380:122-135
- Waxmann SG, Ritchie UM. **Molecular dissection of the myelinated axon.** *Ann Neurol* 1993;33:121-136
- Pinazo-Duran MD, Renau-Piqueras J, Guerri C. **Developmental changes in the optic nerve related to ethanol consumption in pregnant rats: analysis of the aethanol-exposed optic nerve.** *Teratology* 1993;48:305-322
- Sontheimer H, Ritchie UM. **Voltage-gated sodium and calcium channels.** In: Kettenmann H, Ransom BR, eds. *Neuroglia*. New York: Oxford University Press; 1995:202-220
- Nicholson C, Tao L. **Hindered diffusion of high molecular weight compounds in brain extracellular microenvironment measured with integrative optical imaging.** *Biophys J* 1993;65:2277-2290
- Rice M, Okada YC, Nicholson C. **Anisotropic and heterogeneous diffusion in the turtle cerebellum: implications for volume transmission.** *J Neurophysiol* 1993;70:2035-2044
- Szafer A, Zhong J, Gore JC. **Theoretical model for water diffusion in tissues.** *Magn Reson Med* 1995;33:697-712
- Roback H, Scherer H. **Cellular and chemical changes during myelination: histologic, autoradiographic, histochemical and biochemical data on myelination in the pyramidal tract and corpus callosum of rat.** *Virchows Arch Path Anat* 1935;294:265-413
- Arnold G, Holzman E. **Microperoxisomes in the central nervous system of the postnatal rat.** *Brain Research* 1978;155:1-17
- Black JA, Foster RE, Waxman SG. **Rat optic nerve: freeze fracture studies during development of myelinated axons.** *Brain Res* 1982;250:1-21
- Fields R, Waxmann SG. **Regional membrane heterogeneity in premyelinated CNS axons: factors influencing the binding of sterol-specific probes.** *Brain Res* 1988;443:231-242
- Riederer B. **Some aspects of the neuronal cytoskeleton in development.** *Eur J Morphol* 1990;28:347-378
- Watson D. **Regional variation in the abundance of axonal cytoskeletal proteins.** *J Neurosci Res* 1990;30:226-231
- Remahl S, Hildebrand C. **Relations between axons and oligodendroglial cells during initial myelination. I. The glial unit.** *J Neurocytol* 1990;90:313-328
- Lehmenkuhler A, Syklova E, Svoboda J, Zilles K, Nicholson C. **Extracellular space parameters in the rat neocortex and subcortical white matter during postnatal development determined by diffusion analysis.** *Neuroscience* 1993;55:335-351
- Barres BA, Raff MC. **Control of oligodendrocyte number in the developing rat optic nerve.** *Neuron* 1994;12:935-942
- Gargini C, Deplano S, Bisti S, Stone J. **Evidence that the influence of ganglion cell axons on astrocyte morphology is mediated by action spike activity during development.** *Brain Res Dev Brain Res* 1998;110:177-184
- Takigawa T, Hitoshi Y, Kiklaw R, Shigetay Y, Saida T, Kitasato H. **Antibodies against GM1 ganglioside affect  $\text{K}^+$  and  $\text{Na}^+$  currents in isolated rat myelinated fibers.** *Ann Neurol* 1995;37:436-442
- Moll C, Mourre C, Lazdunski M, Ulrich J. **Increase of sodium channels in demyelinated lesions of multiple sclerosis.** *Brain Res* 1991;556:311-316
- Scolding N, Franklin R, Stevens S, Heldin CH, Compston A, Newcombe J. **Oligodendrocyte progenitors are present in the normal adult human CNS and in the lesions of multiple sclerosis.** *Brain* 1998;121:2221-2228
- Stein W. **Channels, Carriers and Pumps. An Introduction to Membrane Transport.** New York: Harcourt Brace Jovanovich Academic Press, Inc; 1990
- Baethmann A, Go K, Unterberg A, eds. **Mechanisms of Secondary Brain Damage.** New York: Plenum Press; 1984
- Utzschneider DA, Thio C, Sontheimer H, Ritchie UM, Waxman SG, Kocsis UD. **Action potential conduction and sodium channel content in the optic nerve of the myelin-deficient rat.** *Proc R Soc Lond B Biol Sci* 1993;254:245-250
- Kato T, Kamada K, Segawa F, et al. **Effects of photo stimulation on the anisotropic diffusion of the visual fibers.** Presented at the 11th Annual Meeting of the Society of Magnetic Resonance in Medicine, Berlin, 1992
- Waxman SG. **Sodium channel blockade by antibodies: a new mechanism of neurological disease?** *Ann Neurol* 1995;37:421-423
- McDonald WI. **Rachelle Fishman-Matthew Moore lecture: The pathological and clinical dynamics of multiple sclerosis.** *J Neuropathol Exp Neurol* 1994;53:338-343